Section 1 Publishable executive Summary

Summary

The work to be carried out in the last 18 months dealt with some final activities on modeling and prototyping.

Concerning Modeling activities, at the end of the project the level of comparison between theory and experiments obtained within NANOPHOTO is totally unprecedented, despite the popularity of Plasma-enhanced chemical vapour deposition reactors. With this respect, the modelling work was a real success, producing original models which were demonstrated to nicely agree with experimental findings.

Some common features of the whole modelling work can be given.

The starting point was mainly dedicated to understand which approaches (e.g., tight-binding vs. empirical potentials vs ab initio description of the atomic-scale interactions, 0D vs 2D reactor model, etc.) were best suited to describe the complex, multi-scale physics of nc-Si films grown by LEPECVD. Then models were first applied to idealized situations (i.e., fully crystalline films, and/or isolated nanoclusters), in order to understand the fundamental physics. Only after a satisfactory conclusion of this work the models were applied to real word situations with results full of physical significance.

As a result of these studies, as an example, the structural evolution of nc-Si and nc-Si/a-Si (e.g. crystalline vs. amorphous ratio) was modellised, by accountig for stress effects due to lattice mismatch substrates and the interface atomic mobility under arbitrary temperature/stress conditions determined . As well, the atomistic model of stress-strain relationship was integrated with continuum theory, as a search for possible constitutive equations for mechanical behaviour of nc-Si and amorphous silicon. Notably we found that twin boundaries spontaneously form within the nanograin during the thermally activated growth. This is an important result to understand the experimental data on grains morphology coming from High Resolution Transmission Electron Microscopy (HRTEM) measurements. According to the atomistic results, twin boundaries were found not the result of grains impingement, as initially supposed, rather they form within each crystallite as a result of the growth mechanism.

Eventually it was also shown that the absorption at energies below the mobility edge is controlled by the localized electronic states.It was found found that angular distortions in the bonding network generate pairs of overlapping localized states (geminate pairs) in the valence and

conduction band tails. These angular defects are optically active and control the low energy absorption.

Such optically active defects can be found in the amorphous phase but, they can also occur in the crystalline phase in the case of sub-nanometric grains. Accordingly, subnanometric grains can act as optically active defects.

The electron-wave function confinement effects within the nanocrystalline phase were then studied in details. We concluded that there is no confinement in pure silicon systems. This result is consistent with the calculated valence and conduction bands alignment between amorphous and crystalline phases.

Concerning prototype devices fabrication and characterization, the aim was to fabricate test PIN devices to be used both photovoltaic and light emission devices. Test devices were fabricated on the base of the best results obtained in the growth of intrinsic and doped layers, but the overall result was not satisfactory enough to understand the full potentialities of the devices, which did not present the requested factors (reproducibility, efficiency) expected.

,

Experimental results, modelling

By using a DAC-TB algorithm it was possible to fully characterize the electronic properties of nanocrystalline silicon (pure or hydrogenated) during a finite temperature crystallization. In particular, we were able to calculate global optoelectronic properties, as well as spatially resolved quantities such as the local density of states. From the local density of states it is possible to calculate the bands extrema and in particular the local band offset.

This method made possible an unprecedented comparison between the structural and the optoelectronic properties of large scale nanocrystalline models. We identified an important effect of the **local strain** on the electronic properties of the amorphous regions. In particular, it was found that the tensile strain increases the absorption coefficient.

It was also found that nc-Si does not present quantum confinement effects. Consistently with the absence of quantum confinement, we find that the average optical absorption is a linear combination (LCIA model) of the absorption of the two bulk phases (amorphous and crystalline). In particular, the optical absorption does not depend on the average size of the nanograins.

The effects of the structural defects on the absorption properties were studied in detail. The absorption at energies below the mobility edge is controlled by the localized electronic states. We found that angular distortions in the bonding network generate pairs of overlapping localized states

(geminate pairs) in the valence and conduction band tails. These angular defects are optically active and control the low energy absorption

Such optically active defects can be found also in the amorphous phase.

Another notable result was a reactor-specific model for the plasma discharge-The POLIMI PECVD reactor model was able to predict the local gas phase ionic composition in striking agreement with experimental data,. The good agreement between calculated and measured ionic composition is indicative of the capability of the model to predict also radical species concentrations, since most ionic species (e.g. H+) are generated by secondary reactions involving radical species. (e.g. H), so that radicals concentrations must be known with accuracy in order to be able to compute ionic concentrations. The great advantage of the plasma model developed by POLIMI is that it predicts gas phase radical and ionic compositions not only at the substrate side, were measurements are performed, but also directly over the wafer surface, where the film growth directly takes place.

Experimental results, Prototyping

A pin structure was deposited on a ZnO:Al coated glass substrate growing for p/i layers in one chamber and the n layer on the other to prevent phosphorus contamination.

Then the structuring of the cells was achieved by evaporating metal stacks through a mask which will form the cells back contacts and performing an SF_6/O_2 plasma etching. By using aluminium as last metal layer, we insure that we remove selectively all the non metal covered silicon layers because SF_6 plasma does not etch aluminum neither ZnO. As metal stack we used Ag(1µm)/Al(1µm) which lead to some contact defoliations therefore we chose Ti(50 nm)/Pd(50nm)/Ag(1µm)/Al(1µm). Figure 1 shows a schematic drawing of the cell design and process sequence.

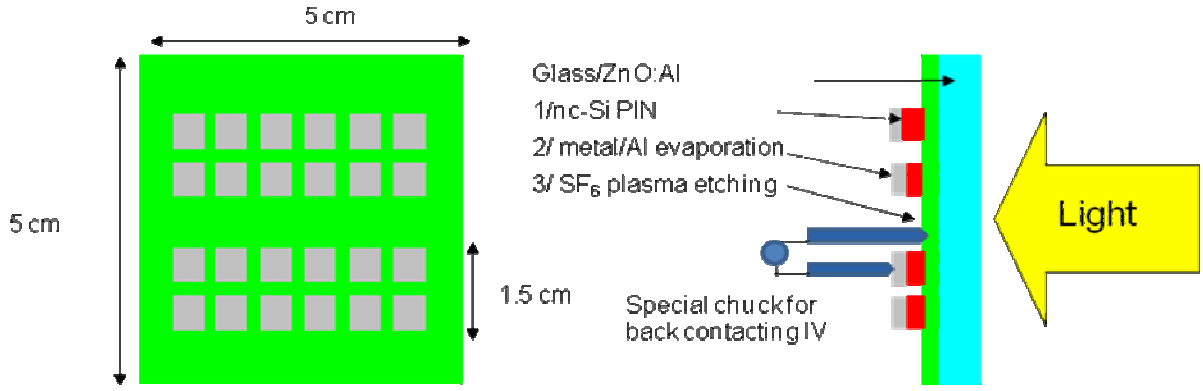

The most important characterization method performed was the IV curves investigation.

Therefore a suitable model has to be used in order to extract meaningful data pertaining to the cell structure and layer quality.

The fundamental difference between pn crystalline solar cells and pin a or nc-Si lies in the way the carrier are collected. The former relies on diffusion while the latter relies on drift which thus implies a strong dependence of the recombination current on the voltage applied that does not exist for c-Si solar cells. Therefore nc-Si cell present a current increase in reverse bias independent from the presence of a parallel resistance due to improved collection when increasing the internal electric field. This difference in the collection mechanism implies additionally that the theoretical diode ideality factor should be 2 for nc-Si pin cells instead of 1 for c-Si pn cells. In practice however a much better fit is obtained considering an ideality factor around 1.5 .

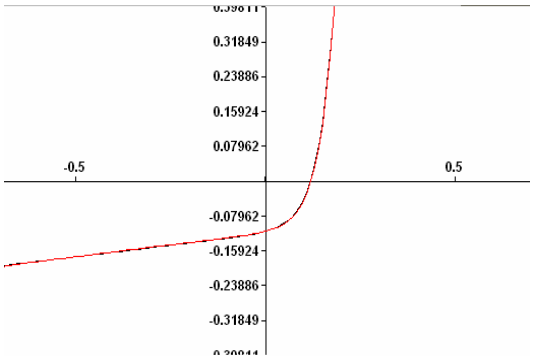

The I-V curves of a typical cell is reported above.

The fitting with the theory model is perfect in its range of validity (reverse bias and low forward bias). We show here a typical IV curve for a working cell of this batch. There is neither series resistance (12 Ωcm²) nor parallel resistance (87000 Ωcm²) problems.

The low value of V_{OC} (118 mV) implied a high J_{on} (4.50 x 10^{-3} mA/cm² with n=1.5) and so a low τ ($J_{on} \propto 1/\tau$) . The low J_{sc} value (0.13 mA/cm²) can be attributed to a too low $\mu_0.\tau_0/\varphi$ value (6.20 x 10^{-10} cm²/V) which is 3 decade lower than literature. for the same kind of cell. Considering in addition that the measured J_{on} value is 3 decade higher than reported in literature,, these results are consistent with a high density of defect in the intrinsic material.